

# The refined 2.0 Å X-ray crystal structure of the complex formed between bovine $\beta$ -trypsin and CMTI-I, a trypsin inhibitor from squash seeds (*Cucurbita maxima*)

## Topological similarity of the squash seed inhibitors with the carboxypeptidase A inhibitor from potatoes

Wolfram Bode, H. Johann Greyling, Robert Huber, Jacek Otlewski\* and Tadeusz Wilusz\*

Max-Planck-Institut für Biochemie, D-8033 Martinsried, FRG and

\*Institute of Biochemistry, University of Wrocław, Tamka 2, 50-137 Wrocław, Poland

Received 7 November 1988

The stoichiometric complex formed between bovine  $\beta$ -trypsin and the *Cucurbita maxima* trypsin inhibitor I (CMTI-I) was crystallized and its X-ray crystal structure determined using Patterson search techniques. Its structure has been crystallographically refined to a final *R* value of 0.152 (6.0 – 2.0 Å). CMTI-I is of ellipsoidal shape; it lacks helices or  $\beta$ -sheets, but consists of turns and connecting short polypeptide stretches. The disulfide pairing is CYS-3I-20I, Cys-10I-22I and Cys-16I-28I. According to the polypeptide fold and disulfide connectivity its structure resembles that of the carboxypeptidase A inhibitor from potatoes. Thirteen of the 29 inhibitor residues are in direct contact with trypsin; most of them are in the primary binding segment Val-2I (P4) – Glu-9I (P4') which contains the reactive site bond Arg-5I – Ile-6I and is in a conformation observed also for other serine proteinase inhibitors.

Serine proteinase inhibitor; Trypsin; Crystal structure; Molecular complex; Carboxypeptidase inhibitor

### 1. INTRODUCTION

Squash proteinase inhibitors form a group of small single-chain proteins (29–32 amino acid residues) thus far exclusively isolated from the seeds of the Cucurbitaceae family [1–4]. On the basis of amino acid sequence, reactive site location and half cystine content they were established as a new family of serine proteinase inhibitors [5–8]. They are the smallest known protein inhibitors of serine proteinases, are very resistant against heat

or acid denaturation and exhibit strong inhibition towards trypsin. The reactive site peptide bond was located in the amino-terminal part of the molecule between Arg-5I or Lys-5I and Ile-6I [9].

CMTI-I is a characteristic representative of the squash inhibitors. It was originally found in seeds of pumpkin (*Cucurbita maxima*), but later also in seeds of figleaf gourd (*Cucurbita ficifolia*) [1]. CMTI-I consists of 29 amino acid residues [5] with Arg-5I (P1) and Ile-6I (P1') constituting the reactive site bond. It binds to bovine  $\beta$ -trypsin with an association constant of  $3.2 \times 10^{11} \text{ M}^{-1}$  [6].

The spatial structure of the squash seeds inhibitors has not yet been elucidated and the disulfide connectivity remained undetermined. In the following we report the crystal structure of a complex of CMTI-I formed with bovine  $\beta$ -trypsin. The detailed structure and a comparison with

Correspondence address: W. Bode, Max-Planck-Institut für Biochemie, D-8033 Martinsried, FRG

Abbreviations: CMTI, *Cucurbita maxima* trypsin inhibitor; CPI, carboxypeptidase A inhibitor from potatoes; rms, root-mean-square; *B*, isotropic temperature factor; Inhibitor residues are indicated by an I after the residue number

related complexes will be communicated elsewhere.

## 2. MATERIALS AND METHODS

CMTI-I was isolated from the seeds of *C. ficifolia* and purified as described [10]. Bovine  $\beta$ -trypsin was purified from commercial trypsin (Merck, Darmstadt) [11,12]. A stoichiometric complex between CMTI-I and bovine  $\beta$ -trypsin was formed by adding both components at a 1.2:1 molar ratio ( $5 \times 10^{-4}$  M). This complex crystallized at 20°C in 20% poly(ethylene glycol) 6000 (Serva, Heidelberg), buffered with 0.1 M phosphate to pH 4–5, using the hanging drop vapour diffusion technique. The crystals are of orthorhombic space group  $P2_12_12_1$ ; the cell constants are  $a = 59.28 \text{ \AA}$ ,  $b = 55.47 \text{ \AA}$ ,  $c = 74.59 \text{ \AA}$ ,  $\alpha = \beta = \gamma = 90^\circ$ . The crystals contain one (complex) molecule per asymmetric unit and diffract to almost 1.8  $\text{\AA}$  resolution.

X-ray intensity data were collected with a FAST television area detector diffractometer (Enraf-Nonius, Delft) using a crystal-to-detector distance of 40.5 mm and a detector angle of 10°. One single crystal was mounted in 2.5 M phosphate buffer, pH 5, and rotated for 95° about  $a^*$  and about an axis 30° oblique to  $a^*$ , respectively. The reflection data (table 1) were evaluated on-line using the program MADNES [13]. The data were corrected for absorption effects using equivalent reflections to determine the absorption ellipsoid of the crystal (using programs of R. Huber and M. Schneider following the theoretical analysis presented [14]) whereafter the Friedel mates were independently averaged and by means of PROTEIN [15] loaded and averaged (table 1).

The orientation of the trypsin component was determined by the rotation function in Patterson space using a model Patterson map (2500 highest peaks, 3–15  $\text{\AA}$  shell) calculated with the refined bovine trypsin model [16] and the crystal Patterson map (calculated with intensity data from 8 to 3.5  $\text{\AA}$ ). The highest peak corresponding to the correct solution was  $7\sigma$  above the mean. The positioning of the trypsin molecule in the unit cell was achieved by a translation function search with programs written by E.E. Lattmann (modified by J. Deisenhofer and R. Huber), and using intensity data from 8 to 3.5  $\text{\AA}$ . The translation function showed highest peaks in the three Harker sections at consistent locations. The rotational and translational parameters were further refined with the Fourier transform fitting program TRAREF [17].

A 3  $\text{\AA}$   $2F_o - F_c$  Fourier map calculated with Sim-weighted

Table 1  
Reflection data

Maximal resolution	2.0 $\text{\AA}$
Number of measurements	54864
$R_{\text{merge}}^a$ after scaling and absorption correction	0.073
$R_{\text{merge}}^a$ of Friedel mates	0.036
Number of independent reflections	14191
Measured/possible reflections to 2 $\text{\AA}$	0.81

<sup>a</sup>  $R_{\text{merge}} = \sum(I - \langle I \rangle)/\sum I$

Table 2  
Final model parameters of the CMTI-trypsin structure

Number of active protein atoms	1818
Number of inactive protein atoms	16
Number of active solvent atoms	140
rms standard deviation from target values	
Bond lengths	0.020 $\text{\AA}$
Bond angles	2.70°
Total internal energy	-1325 kcal/mol
Resolution range	6.0–2.0 $\text{\AA}$
Number of unique reflections used for refinement	13077
$R$ value	0.151 <sup>a</sup>
Mean $B$ value	15.0 $\text{\AA}^2$
Lower $B$ value limit	3.0 $\text{\AA}^2$
Estimated mean coordinate error from agreement between observed and calculated structure factors	
According to Luzzati [34]	0.18 $\text{\AA}$
According to Cruickshank [35]	0.14 $\text{\AA}$

<sup>a</sup> Rejecting 1.5% of all reflections with  $2(|F_o| - |F_c|)/(|F_o| + |F_c|) > 1.2$

model phases displayed the trypsin molecule and in addition showed electron density representing the inhibitor. The complete CMTI-I polypeptide chain was modeled into the electron density on a PS330 interactive display (Evans and Sutherland) using the PSFRODO version [18] of FRODO [19]. The enzyme-inhibitor model was refined within 7 macrocycles using the energy restraint crystallographic refinement EREF [20] and energy parameters mentioned recently [21]; all non-bonded restraint parameters for Ser-195 O<sub>γ</sub> were set to zero to allow its unbiased approach to the reactive site bond of the inhibitor. Between every two macrocycles Fourier and difference Fourier maps were inspected at the graphics display to correct gross model errors.

The intensity data used were gradually extended to 2.0  $\text{\AA}$  resolution. Solvent molecules were inserted at stereochemically reasonable positions if the difference electron density exceeded  $4\sigma$ . Finally, individual  $B$  values were also refined. The final  $R$  value (defined as  $\sum(|F_o| - |F_c|)/\sum |F_o|$  for 13077 reflections between 6.0 and 2.0  $\text{\AA}$  resolution is 0.151. The final refinement characteristics are given in table 2.

## 3. RESULTS

Fig.1 shows an  $\alpha$ -carbon drawing of the CMTI-I-bovine trypsin complex, with the inhibitor bound to the substrate binding cleft and projecting from the enzyme as a relatively small hump. The trypsin chain can be completely traced in the Fourier map from Ile-16 down to Asn-245, with only 12 side



Fig.1.  $\alpha$ -Carbon drawing of the complex formed between bovine  $\beta$ -trypsin (thin connections) and CMTI-I (bold connections). For sake of simplicity, only the residues of the tryptic active site triad, Asp-189 (S1-pocket) and the C-terminal Asn-245 of trypsin and P1-residue Arg-51 of CMTI-I are given in full detail.

chain atoms remaining undefined due to higher mobility. Main chain segments 74–79 (forming part of the 'calcium-loop' in trypsin [16]), 146–149 (being part of the 'autolysis loop' which contains the primary cleavage site for autodigestion [11]) and 243–245 (carboxy terminus) exhibit  $B$  values significantly above the mean. The 'calcium-site' is only very weakly occupied (interpreted as solvent molecule Sol-944, with extremely short contacts to Val-75 O); the low occupancy gives rise to the relatively large disorder of this loop [16]. The trypsin conformation is very weakly affected by inhibitor binding or by the different cell contacts; the rms deviation of all  $\alpha$ -carbon atoms of the trypsin component compared with free or benzamidine liganded bovine trypsin is 0.34 Å, i.e. only slightly above the estimated coordinate errors (table 2). As usually observed for serine proteinase complexes the active site residues and most segments comprising the binding site are optimally superimposable. All internal and many of the surface bound solvent molecules occupy identical positions.

The inhibitor (fig.2) roughly exhibits the shape of a flat-iron, with the base plate made up of the polypeptide chain from Met-8I on, and the grip formed by the protruding reactive site loop containing the scissile peptide bond Arg-5I–Ile-6I. The essentially hydrophobic side chains of this loop (Pro-4I, Ile-6I, Leu-7I, Met-8I) make up together with Val-2I, Tyr-27I, Leu-17I and Ala-18I a curved shell of hydrophobic surface, which

passes over continuously into the hydrophobic core formed by the adjacent disulfide bridges traversing the center of the molecule. The half-side open cavity of mixed hydrophobic and polar character is filled with 3 strongly fixed solvent molecules of extremely low  $B$  values, namely Sol-919, Sol-808, and Sol-915, which might be considered as integral constituents of the structure (fig.2). The molecular surface of the inhibitor opposite to the binding loop comprises more polar and charged residues; a few loop segments, such as the relatively mobile turn around Glu-24I and His-25I, emerge from the surface.

With the exception of two tight turns the inhibitor polypeptide chain lacks any regular extended secondary structure elements. Due to main chain conformation and intramolecular hydrogen bonding, the inhibitor peptide chain can be subdivided into the following segments (fig.3): (i) the extended curved proteinase binding loop Arg-1I–Met-8I; (ii) an extended segment Met-8I–Lys-11I; (iii) a short irregular  $3_{10}$ -helix of 1½ turns from Lys-12I to Cys-16I; (iv) a type-II' tight turn from Leu-17I to Cys-20I; (v) segment Cys-20I–Leu-23I of extended conformation; (vi) a tight turn of approximately type I from Leu-23I to Gly-26I; (vii) the extended carboxy-terminal segment Gly-26I–Gly-29I.

Type II'-turns usually have glycines at their second positions [22]; indeed, Ala-18I in the Leu-17I–Cys-20I turn is outside of the normally

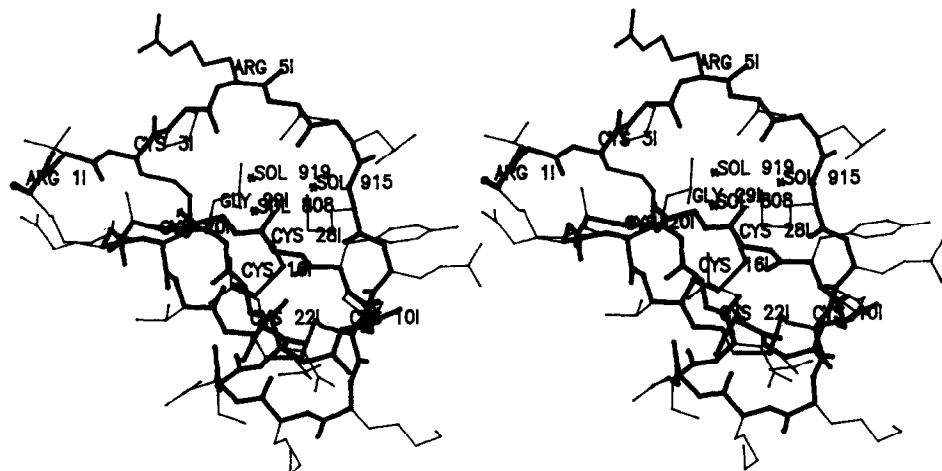


Fig.2. Complete structure of CMTI-I. Main chain atom connections and disulfide bridges are emphasized by bold lines. Only the 'internal' solvent molecules Sol-808, Sol-915 and Sol-919 are shown.

'allowed'  $\phi$ - $\psi$ -region and in a strained conformation ( $\phi = 55^\circ$ ,  $\psi = -127^\circ$ ).

There are only a few intramolecular hydrogen bonds in CMTI-I (fig.3). All parts of the polypeptide chain, including the amino and the carboxy termini, are rather uniformly crosslinked with one

another through the three disulfide bridges (figs 2 and 3). The disulfide pairing is Cys-3I-Cys-20I, Cys-10I-Cys-22I and Cys-16I-Cys-28I, i.e. the three cysteine residues of the amino-terminal half are connected with those of the carboxy terminal half in identical order. The first two disulfide bridges are of right-handed, the third one is of left-handed conformation. All three disulfide bridges are arranged side by side, with Cys-16I-Cys-28I located in the middle.

The amino and the carboxy-terminal ends are localized at the same side of the inhibitor molecule, but still almost 10 Å apart from one another (fig.2). The amino terminus points away from the molecule and lacks any visible hydrogen bond partner. The side chain of Arg-1I is bent backwards to the molecular center; its guanidyl group counterbalances the carboxylate group of Gly-29I and forms slightly asymmetrically two hydrogen bonds. The Arg-1I side chain is further hydrogen bonded (through Glu-19I O) with segment Glu-19I-Val-21I, which in turn is connected through two hydrogen bonds with Gly-29I (see fig.3). In this way amino and carboxy termini are fixed to the molecular core; the compact structure may further contribute to the resistance against proteolytic attack by exoproteases. On the opposite side of the inhibitor molecule Asp-15I is likewise engaged in a surface-located salt bridge with the side chain of Lys-12I, and simultaneously

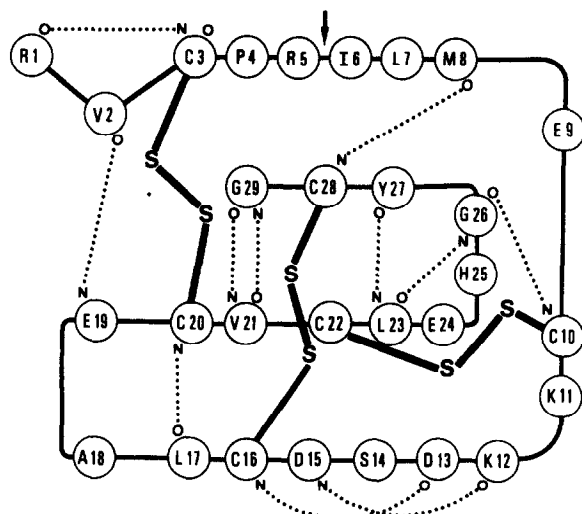


Fig.3. Schematic representation of the polypeptide arrangement of CMTI-I and its disulfide connectivities. Inter-main-chain hydrogen bonds displayed by dashed lines were selected according to definitions (using energy cut-off values of  $-1.0$  kcal/mol) given by Kabsch and Sander [36]. The arrow indicates the scissile peptide bond.

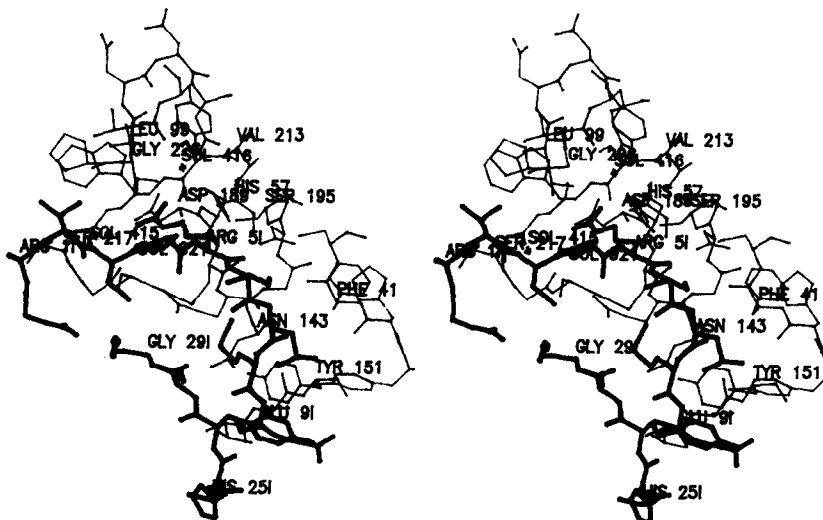


Fig.4.  $\beta$ -Trypsin-CMTI-I interface. Polypeptide chain segments of CMTI-I are given by bold lines, trypsin segments by thin lines.

suitably placed to counterbalance the amide dipoles of Lys-11I and Lys-12I (see fig.2).

The proteinase binding loop of CMTI-I is between Cys-3I (P3) and Met-8I (P3') in a similar conformation to that observed in the other 'small' serine proteinase protein inhibitors known so far [21,23], whereas the remainder of CMTI-I is organized in a completely different fold. The rms deviation of the  $\alpha$ -carbon atoms from Cys-3I to Leu-7I compared with the equivalent atoms of Arg15-BPTI in the trypsinogen complex [24] is, for example, 0.56 Å. The CMTI-I reactive site loop appears to be tensed between disulfide bridges Cys-3I-Cys-20I and Cys-10I-Cys-22I. Its central part, around the intact scissile peptide bond Arg-5I-Ile-6I, is linked via Sol-919 (fig.2) with the center of the molecule. In this respect the squash inhibitors differ from the other inhibitors where the reactive site is clamped to the core through main or side chain hydrogen bond interactions. Sol-919 in CMTI-I occupies a site equivalent to Asn-33I N $\delta$ 2 in ovomucoid third domains [25].

Fig.4 gives a section of the CMTI-I-trypsin interface. There are 138 intermolecular nonhydrogen atom-atom contacts below 4.0 Å, all but 7 made by the 8 residues Arg-1I to Leu-7I and Glu-9I of the primary binding segment. The few residual contacts are made by the carboxy-terminal residues His-25I to Gly-29I. The main chain atoms from Cys-3I to Met-8I exhibit (besides all cysteine

residues) the smallest  $B$  values observed in the whole inhibitor molecule. In almost half of the contacts P1-residue Arg-5I is involved. Its side chain is accommodated in the S1-pocket of trypsin virtually identical to the geometry observed for Arg-15I in the Arg15-BPTI-trypsinogen complex [24], with its distal guanidyl group engaged in a salt bridge with Asp-189 and further hydrogen bonded to Gly-219 O and to an internal solvent molecule (Sol-416). As usually observed in serine proteinase-inhibitor complexes the primary binding segment of CMTI-I runs antiparallel to trypsin segment Ser214-Gly216, and intermolecular main chain-main chain hydrogen bonds are possible between Cys-3I (P3) and Gly-216, between Arg-5I (P1) and Ser-214, Gly-193 and Ser-195, and between Leu-7I and Phe-41. Remarkable is the weakness of the first hydrogen bond pair at P3-S3 and the relatively short and stereochemically favourable hydrogen bond between Arg-5I N and Ser-214 O. In agreement with the observation for other complexes, the scissile peptide bond Arg-5I-Ile-6I is intact and almost planar, and its carbonyl carbon is in van der Waals contact with Ser-195 O $\gamma$  (fig.4).

#### 4. DISCUSSION

This crystal structure analysis for the first time revealed the spatial organization of the polypep-

ptide chain of a squash seed inhibitor. In agreement with proposals derived from CD-measurements [26], these inhibitors lack any regular secondary structure elements. Similar to the other 'small' protein inhibitors directed against serine proteinases, the 'primary' binding segment (around the reactive site bond Arg-5I–Ile-6I) protrudes from the main molecular body in a characteristic conformation allowing an intimate contact with the cognate enzyme. In spite of different size and fold of the squash inhibitors the interaction pattern is similar to that observed in other related complexes.

A remarkable feature of CMTI-I is the ion pair interaction of the Arg-1I side chain with the carboxy terminus and the hydrogen bond linkage of both groups to the molecular core. In contrast to inhibitors isolated from *Cucurbita* seeds (i.e. with an Arg-1I), all inhibitor species from *Cucumis* seeds analyzed so far possess a methionine residue at the homologous position 1. These natural variants offer the possibility to estimate the significance of the salt bridge. According to <sup>1</sup>H-NMR studies [27] the inhibitors from *Cucurbita* seem to be more rigid than those from *Cucumis*, in agreement with the idea that this salt bridge promotes stability. This hypothesis might be further tested by following the thermal denaturation of these different inhibitor species or by a comparison of the thermal behaviour of Lys-5I-containing inhibitors from *Cucurbita* before and after arginine modification by means of cyclohexanedione [10].

On the other hand, the inhibitors from *Cucumis* seeds (i.e. with Met-1I) or variants with elongated carboxy termini [6] exhibit comparable inhibitory activity, indicating that salt bridge formation is not essential for function. The elongated variants frequently observed [6] let one assume that the 29-mer studied here is the result of posttranslational trimming at one or both ends.

An important contribution to stability of these small inhibitors comes from the three disulfide bridges, which knit together all parts of the polypeptide chain. This structure analysis established the correct disulfide connectivity with the first three cysteine residues being covalently linked with the last three in consecutive order (this disulfide pairing has now been independently confirmed by mass spectroscopy by Stachowiak, Otlewski, Polanowski and Dyckes, manuscript in preparation). Led by the number and sequence of these cysteines, Siemion et al. [27] had speculated about the possible similarity with each of the four domains of wheat germ agglutinin isolectin 2 [28]. CMTI-I exhibits an identical disulfide pairing for the first six cysteines (in disagreement with the connectivity proposed for squash seed inhibitors [27]) and a very weak topological resemblance of the amino-terminal half of CMTI-I with part of the first wheat germ agglutinin domain and with a few other structurally related 'four-disulfide core proteins' [29].

Much more evident (fig.5), in contrast, is the structural relation of CMTI-I with the carboxypep-

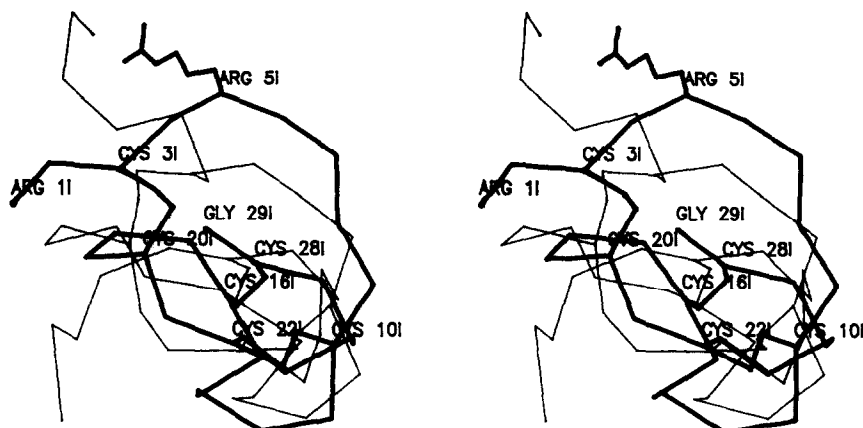


Fig.5.  $\alpha$ -Carbon drawing of CMTI-I (bold lines) overlaid with the CPI model (30) (thin lines). The disulfide bridges of both models are indicated, and P1-residue Arg-5I is shown with all nonhydrogen atoms.

tidase A inhibitor from potatoes (CPI) [30]. In particular, the six cysteine residues and the connecting disulfide bridges occupy quite analogous positions in both molecules; the rms deviation of the corresponding six  $\alpha$ -carbon atoms amounts to 1.8 Å. From the second cysteine on (Cis-10I in CMTI-I), the polypeptide fold is quite similar. The amino-terminal reactive site loop of the squash seed inhibitor finds no counterpart in CPI; the CPI-chain exhibits here a less prominent loop. On the other hand, the CPI chain is elongated on both ends, with the carboxy terminus being the exoprotease binding site [30]. A sequence alignment made according to the superposition shown in fig.5 yields (besides the six cysteines) only four identical residues. The topological similarity nevertheless suggests a common evolutionary origin of both molecules.

The squash inhibitors seem to be particularly attractive candidates for remodeling their affinity and specificity properties. Their small size makes them well suited for total chemical synthesis. CMTI-III has previously been made by solid-phase synthesis methods [31]. Very recently a P1-valine analogue of CMTI-III was synthesized which exhibited high inhibitory activity towards human leukocyte elastase [32]. The fit to this latter enzyme of tremendous therapeutic interest is conceivable from a hypothetical complex modeled with the leucocyte elastase structure [33]. Analogous exchanges could yield inhibitors of still different specificity. Knowing the detailed interaction with cognate enzymes, residues more remote from the reactive site could be changed in a systematic manner, yielding inhibitors with improved affinity properties or higher selectivity. Alternatively, the squash seed inhibitor chain could be elongated on the carboxy terminus to make it a carboxypeptidase inhibitor. Generally these inhibitors could be utilized as simple design motives to create new functions.

**Acknowledgements:** We thank I. Mayr for skillful help with crystallization. The receipt of grants from the Alexander-von-Humboldt-Stiftung (H.J.G.), from the Polish Academy of Sciences (grant CPBR 3.13.6 to J.O. and T.W.) and from the Fond der Chemischen Industrie (W.B.) is greatly appreciated. This work has been supported by the Sonderforschungsbereich 207 of the Deutsche Forschungsgemeinschaft (grant H-1 to W.B. and H-2 to R.H.).

## REFERENCES

- [1] Polanowski, A., Cieslar, E., Otlewski, J., Nienartowicz, B., Wilimowska-Pelc, A. and Wilusz, T. (1987) *Acta Biochim. Polon.* 34, 395–406.
- [2] Polanowski, A., Otlewski, K., Leluk, J., Wilimowska-Pelc, A. and Wilusz, T. (1988) *Biol. Zentralbl.* 107, 45–49.
- [3] Hojima, Y., Pierce, J.V. and Pisano, J.J. (1982) *Biochemistry* 21, 3741–3746.
- [4] Joubert, F.J. (1984) *Phytochemistry* 7, 1401–1406.
- [5] Wilusz, T., Wieczorek, M., Polanowski, A., Denton, A., Cook, J.I. and Laskowski, M., jr (1983) *Hoppe Seyler's Z. Physiol. Chem.* 364, 93–95.
- [6] Wieczorek, M., Otlewski, J., Cook, J., Parks, K., Leluk, J., Wilimowska-Pelc, A., Polanowski, A., Wilusz, T. and Laskowski, M., jr (1985) *Biochem. Biophys. Res. Commun.* 126, 646–653.
- [7] Laskowski, M., jr and Kato, I. (1980) *Annu. Rev. Biochem.* 49, 593–626.
- [8] Otlewski, J., Whatley, H., Polanowski, A. and Wilusz, T. (1987) *Biol. Chem. Hoppe-Seyler* 369, 1505–1507.
- [9] Nowak, K., Slominska, A., Polanowski, A., Wieczorek, M. and Wilusz, T. (1981) *Hoppe-Seyler's Z. Physiol. Chem.* 362, 1017–1019.
- [10] Otlewski, J., Polanowski, A., Leluk, J. and Wilusz, T. (1984) *Acta Biochim. Polon.* 31, 267–278.
- [11] Schroeder, D.D. and Shaw, E. (1968) *J. Biol. Chem.* 243, 2943–2949.
- [12] Fehlhammer, H. and Bode, W. (1975) *J. Mol. Biol.* 98, 683–692.
- [13] Messerschmidt, A. and Pflugrath, J.W. (1987) *J. Appl. Crystallogr.* 20, 306–315.
- [14] Kopfmann, G. and Huber, R. (1968) *Acta Crystallogr. A24*, 348–351.
- [15] Steigemann, W. (1974) PhD Thesis, TU München.
- [16] Bode, W. and Schwager, P. (1975) *J. Mol. Biol.* 98, 693–717.
- [17] Huber, R. and Schneider, M. (1985) *J. Appl. Crystallogr.* 18, 165–169.
- [18] Pflugrath, J.W., Saper, M.A. and Quiocho, F.A. (1984) in: *Methods and Application in Crystallographic Computing* (Halls, S. and Ashiaka, T. eds) p.407, Clarendon Press, Oxford.
- [19] Jones, T.A. (1978) *J. Appl. Crystallogr.* 11, 268–272.
- [20] Jack, A. and Levitt, M. (1978) *Acta Crystallogr. A345*, 931–935.
- [21] Bode, W., Papamokos, E. and Musil, D. (1987) *Eur. J. Biochem.* 166, 673–692.
- [22] Crawford, J.L., Lipscomb, W.N. and Schellman, C.G. (1973) *Proc. Natl. Acad. Sci. USA* 70, 538–542.
- [23] Read, R.J. and James, M.N.G. (1986) in: *Proteinase Inhibitors* (Barrett, A.J. and Salvesen, G. eds) pp.301–336, Elsevier, Amsterdam.
- [24] Bode, W., Walter, J., Huber, R., Wenzel, H.R. and Tschesche, H. (1984) *Eur. J. Biochem.* 144, 185–190.
- [25] Papamokos, E., Weber, E., Bode, W., Huber, R., Empie, M.W., Kato, I. and Laskowski, M., jr (1982) *J. Mol. Biol.* 158, 515–537.

- [26] Szewszuk, A., Kurowska, E., Prusak, E., Wilusz, T., Polanowski, A., Otlewski, J., Solczyk, J. and Siemion, I.Z. (1983) *Hoppe-Seyler's Z. Physiol. Chem.* 364, 941-947.
- [27] Siemion, I.Z., Wilusz, T. and Polanowski, A. (1984) *Mol. Cell. Biochem.* 60, 159-161.
- [28] Wright, C.S. (1987) *J. Mol. Biol.* 194, 501-529.
- [29] Drenth, J., Low, B.W., Richardson, J.S. and Wright, C.S. (1980) *J. Biol. Chem.* 255, 2652-2655.
- [30] Rees, D.C. and Lipscomb, W.N. (1982) *J. Mol. Biol.* 160, 475-498.
- [31] Kuprysiewski, J., Ragnarsson, W., Rolka, K. and Wilusz, T. (1986) *Int. J. Peptide Protein Res.* 27, 245-250.
- [32] Rolka, K., Kuprysiewski, G., Ragnarsson, W., Otlewski, J., Wilusz, T. and Polanowski, A. (1989) *Int. J. Peptide Protein Res.*, submitted.
- [33] Bode, W., Wei, A.-Z., Huber, R., Meyer, E., Travis, J. and Neumann, S. (1986) *EMBO J.* 5, 2453-2458.
- [34] Luzzati, V. (1952) *Acta Crystallogr.* 5, 802-810.
- [35] Cruickshank, D.W.J. (1949) *Acta Crystallogr.* 2, 65-82.
- [36] Kabsch, W. and Sander, C. (1983) *Biopolymers* 22, 2577-2637.